

## Skeletal muscle myosin subfragment 1 dimers

Karen Claire<sup>a</sup>, Robert Pecora<sup>a</sup>, Stefan Highsmith<sup>b,\*</sup>

<sup>a</sup> Department of Chemistry, Stanford University, Stanford, CA 94305, USA

<sup>b</sup> Department of Biochemistry, School of Dentistry, University of the Pacific, San Francisco, CA 94115, USA

Received 30 August 1996; revised 12 September 1996; accepted 12 September 1996

### Abstract

The rate of translational diffusion of skeletal muscle myosin subfragment 1 (S1) was determined from polarized dynamic light scattering autocorrelation measurements. Diffusion rates were expressed in terms of the hydrodynamic radii  $R_h$ . At 20 °C, in low ionic strength pH 8 solutions,  $R_h$  increased from 4.3 nm to 5.7 nm as [S1] was increased from 1.6 to 72  $\mu$ M. Including MgATP to maintain  $S1 \cdot MgADP \cdot P_i$  gave equivalent results. When the light scattering data were analyzed, assuming a monomer–dimer equilibrium, a dissociation constant of 83  $\mu$ M was obtained. Steady state MgATPase activity measurements were made as a function of [ATP] for S1 in the 0.4–7  $\mu$ M range, and analyzed assuming Michaelis–Menten kinetics.  $V_{MAX}$  did not change, but  $K_M$  increased about tenfold as [S1] was increased over this range. The light scattering and kinetic data were consistent with S1 aggregation at high [S1].

**Keywords:** ATP; ATPase; Dimerization; Light scattering; Myosin subfragment 1

### 1. Introduction

The structure of type-two myosins consists of an elongated heavy-chain domain made of a coiled-coil of two  $\alpha$ -helices, at the end of which are two globular motor domains. Each motor domain comprises part of one heavy chain plus two light chains. A myosin motor domain is called a “head” when it is part of myosin, or subfragment 1 (S1) when it is

isolated as a proteolytic fragment. This duplex structure of the myosin molecule suggests that interaction may occur between the two motor domains. The possible inter-head interactions fall into three categories: the production of force, the maintenance of processivity and the regulation of activity.

There is good evidence that a single head of myosin can use ATP to produce force while bound to actin. Threads made of single-headed myosin and actin can shorten and produce force [3]. Isolated S1 can also use ATP to move actin [4]. The presence of the regulatory light chain on S1 increases the movement of actin [5]. However, S1 itself is sufficient for movement or force production, and head–head interactions are not required.

The second possibility, that interaction between the two heads of myosin may be required for processivity (to maintain attachment to actin), arises be-

Abbreviations: CONTIN, a computer program used to analyze decay data [1,2];  $K_D$ , dissociation constant;  $K_M$ , Michaelis–Menten constant;  $L$ , length of molecule;  $n$ , index of refraction;  $q$ , scattering vector length;  $R_h$ , hydrodynamic radius of spherical particle determined from translational diffusion; S1, myosin subfragment 1;  $\eta$ , solution viscosity;  $\theta$ , angle of scattered intensity from the transmitted beam;  $\lambda$ , wavelength of light;  $\tau$ , decay time for relaxation of scattered intensity from autocorrelation function

\* Corresponding author.

cause each head spends part of the ATP hydrolysis cycle dissociated [6]. A related motor protein with a duplex structure, kinesin, appears to require interaction between its two heads for motility on a microtubule. The high processivity of kinesin is maintained either by allosteric communication between the two heads [7], or by diffusion of one head during the time the second is bound [8,9]. An individual kinesin head can function as a motor, but high processivity is required to keep the kinesin bound to the microtubule. Myosin, on the other hand, appears to have low processivity [10]. It is likely that the supramolecular arrays of actin and myosin in muscle maintain processivity, making kinesin-like head-head interactions for an individual myosin unnecessary.

The third possibility, that the heads of myosin interact as part of a regulatory mechanism, does have some support. For example, smooth muscle may be inhibited by a physical interaction between the heads, which occurs when the regulatory light chains in the motor domain are not phosphorylated [11,12]. Consistent with the idea that the heads of smooth muscle myosin interact functionally, they have been chemically crosslinked to one another, suggesting that they are in close proximity [13], and neighboring actin-bound S1 molecules have also been crosslinked by zero-length crosslinkers [14].

There are data suggesting that skeletal muscle myosin heads also interact to modulate their activity, either during ATPase activity by myosin [15] or during *in vitro* motility assays [16]. The interaction of skeletal muscle heads also appears to change when the regulatory light chain is phosphorylated [17]. Relevant to these possible regulation-related head-head interactions by skeletal muscle myosin, the association of S1 in solution and the effects of association on ATPase activity have been reported [18,19]. However, none of these reports on skeletal muscle inter-head functional interactions has been accepted as conclusive, and the possibilities of regulatory interactions between myosin heads, either as part of myosin or isolated in solution, have been ignored in most cases.

In this paper, we report clear physical evidence from polarized dynamic light scattering autocorrelation measurements indicating that skeletal S1 aggregates, under conditions for which corroborating ki-

netic data exist showing that its function is modified by aggregation. It appears that S1 dimers can form under some conditions, and that they have a reduced apparent  $K_M$  for MgATP.

## 2. Materials and methods

### 2.1. Proteins and chemicals

Myosin was isolated from New Zealand rabbit dorsal muscle [20]. Myosin subfragment 1 was prepared from myosin using papain [21] and purified by size exclusion chromatography (Sephacryl S-400) followed by anion exchange chromatography (DE-52) [22]. Experiments were performed using mixtures of S1 with its regulatory light chain plus either essential light chain 1 or essential light chain 2 bound. S1 MgATPase activity was typically  $0.035\text{--}0.049\text{ s}^{-1}$ . The chemicals used to prepare the buffers were of reagent grade.

### 2.2. MgATPase measurements

Steady state MgATPase activities for S1 were determined at  $25^\circ\text{C}$  and pH 8 using a coupled assay system [23].

### 2.3. Light scattering sample preparation

Doubly distilled water was prepared by re-distilling deionized water with a Corning Mega-Pure still. An initial cleaning of the 1 cm square quartz cuvettes was performed by rinsing each cell for a minimum of 24 h with deionized water. To remove dust, each cuvette was next rinsed for a minimum of 24 h with doubly distilled water which was cycled through Gelman Sciences Acrodisc PF filters containing a  $0.8\text{ }\mu\text{m}$  prefilter and a  $0.2\text{ }\mu\text{m}$  Supor filter, using a Monostat Cassette Pump. The cuvettes were inspected for dust by observing a focused 200 mW 488 nm wavelength laser beam in the cuvette under  $5\times$  magnification. If dust was seen, the cuvette was returned to the filtered water rinse system.

Concentrated ATP and buffer solutions were filtered through  $0.2\text{ }\mu\text{m}$  Supor filters, and concentrated S1 solutions were filtered through  $0.45\text{ }\mu\text{m}$  Supor filters, directly into a clean cuvette immediately be-

fore a measurement was begun. The cuvette was weighed using an analytical balance before and after each addition to determine the dilution. In some cases, if dust was detected in a sample, the loaded cuvette was centrifuged at  $4000 \text{ rev min}^{-1}$  in a Sorvall RC-5B centrifuge for 1–2 h.

#### 2.4. Light scattering measurements

The optics of the light scattering apparatus were of standard design and have been described elsewhere [24]. The wavelength of the light was 488 nm. The power was 200 mW. Photon correlation functions were measured using a Brookhaven Model BI-9000AT digital correlator. The variable delay channel settings were ratio spaced to include from 2 to 10000  $\mu\text{s}$  in order to increase the range of decay times available for analysis. Scattered light intensities were measured at  $33.00^\circ$ ,  $57.00^\circ$  and  $90.00^\circ$  from the transmitted beam. Only data with measured and calculated baseline percentage differences of less than 0.10% were used for analyses. Data were transferred to a VAXStation 3200 using VMS Kermit-32 version 3.5.051 for analysis with the Fortran program CONTIN [1,2].

### 3. Results

Steady state MgATPase activities at  $25^\circ\text{C}$  in 10 mM KCl, 10 mM Tris, 2 mM  $\text{MgCl}_2$ , 0.25 mM EDTA and 0.100 mM MgATP (pH 8) were measured for solutions containing increasing [S1]. The data were analyzed to obtain  $V_{\text{MAX}}$  and  $K_{\text{M}}$ , assuming Michaelis–Menten kinetics. The values for  $V_{\text{MAX}}$  ( $0.042 \pm 0.007 \text{ s}^{-1}$ ) were independent of [S1], but  $K_{\text{M}}$  increased about tenfold as [S1] increased in the  $0.4\text{--}7 \mu\text{M}$  range (Fig. 1). The increase in  $K_{\text{M}}$  with [S1] for a particular S1 preparation was comparable with the variations in  $K_{\text{M}}$  observed using different S1 preparations in some cases. However, the increase in  $K_{\text{M}}$  was consistently reproducible for a given S1 preparation, and typically increased tenfold in the [S1] range used (Fig. 2).

It is difficult to rationalize the observed dependence of  $K_{\text{M}}$  on [S1] without invoking some physical interaction between S1 molecules, presumably some degree of S1 aggregation. To explore this

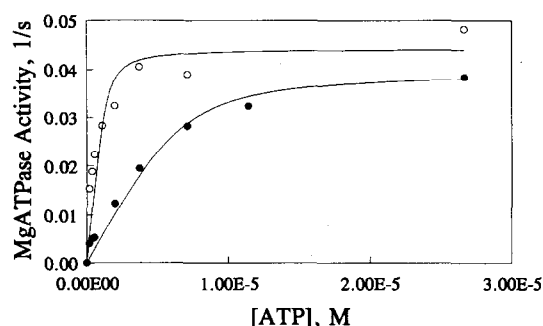


Fig. 1. Steady state MgATPase activity. The activity of S1 at  $25^\circ\text{C}$  in 10 mM KCl, 10 mM Tris, 2 mM  $\text{MgCl}_2$  and 0.25 mM EDTA (pH 8) and increasing [ATP] was measured using a coupled assay technique. [S1]:  $1.3 \mu\text{M}$  (○);  $6.6 \mu\text{M}$  (●). The full curves are the best fits to the data assuming Michaelis–Menten kinetics to obtain values for  $V_{\text{MAX}}$  and  $K_{\text{M}}$ .

interpretation of the kinetic data, polarized dynamic light scattering time correlation measurements were made on solutions containing increasing [S1] or  $[\text{S1} \cdot \text{MgADP} \cdot \text{P}_i]$  in order to estimate the rates of translational diffusion. If aggregates are formed, they will be expected to diffuse more slowly than S1 monomers.

The scattered intensity autocorrelation function was measured for solutions containing  $1.6\text{--}72 \mu\text{M}$  S1 in 10 mM KCl, 10 mM Tris (pH 8), 2 mM  $\text{MgCl}_2$  and 0.25 mM EDTA at  $20^\circ\text{C}$ , and analyzed to obtain the decay rates of the autocorrelation function. In some experiments, MgATP was included at concentrations high enough (5–20 mM MgATP) to maintain  $\text{S1} \cdot \text{MgADP} \cdot \text{P}_i$  during the measurement.

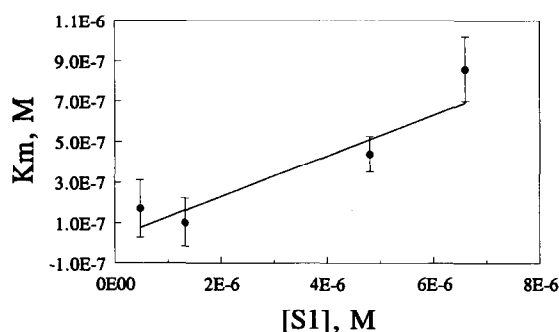


Fig. 2.  $K_{\text{M}}$  vs. [S1].  $K_{\text{M}}$  values, from the fitting of the Michaelis–Menten equation to the steady state ATPase activities, are plotted for several [S1] values. The conditions are given in Fig. 1.

An ATP regenerating system was not used in order to avoid light scattering from the enzymes required for the system. The autocorrelation function was analyzed as a distribution of diffusion rates contributing to the decay using the program CONTIN [1,2].

Diffusion rates obtained using CONTIN were expressed in terms of an average hydrodynamic radius  $R_h$  (Fig. 3).  $R_h = q^2 \tau kT / 6\pi\eta$  is the radius of a sphere of the size predicted by the Stokes–Einstein relation to translate with a diffusion rate corresponding to the decay rate of the peak, where  $q$  is the scattering vector length,  $\tau$  is the decay time of the relaxation,  $k$  is Boltzmann's constant,  $T$  is the temperature and  $\eta$  is the solvent viscosity.  $q = (4\pi n/\lambda) \sin(\theta/2)$ , where  $n$  is the refractive index of the solution,  $\lambda$  is the wavelength of the scattered light and  $\theta$  is the scattering angle. The number of particle sizes (i.e.  $R_h$  values) needed to best fit the data is a variable parameter in this method of analysis. For S1, this number is almost always unity (Fig. 3), but the value of  $R_h$  increases with increasing [S1]. This is the result expected if the average size of the scattering particle increases with increasing concentration, but the differences between the smaller and larger particles are too small for their individual decay times to be resolved.

Occasionally, anomalous behavior was observed. Small amplitude peaks (less than 10% of the total intensity) were found at the fast edge of the window of the decay times used for analysis. These features of CONTIN analyses have been observed previously, and are probably artifacts of the analysis [25]. In addition, for some of the solutions containing ATP, a larger amplitude peak (less than 20% of the total intensity) corresponding to very large particles was observed. This "slow mode" signal, which was not investigated further, may be due to dust or to small amounts of very large aggregates of  $S1 \cdot MgADP \cdot P_i$ .

For sufficiently elongated molecules, the polarized dynamic light scattering time correlation function contains contributions from macromolecular translational diffusion and rotational diffusion. The relative contributions of translational and rotational motion depend on the product of the scattering vector length  $q$  and the length of the long axis of the molecule  $L$  [26]. For S1, at all the concentrations used, with and without ATP,  $R_h$  is independent of  $q$ . These data indicate that neither S1 rotation, nor any internal mode of motion, contributes to the decay of the autocorrelation function, as expected for a molecule as small as S1 [26]. For each [S1], the data for all angles were averaged to obtain an  $R_h$  value which derives from the rate of translational diffusion.

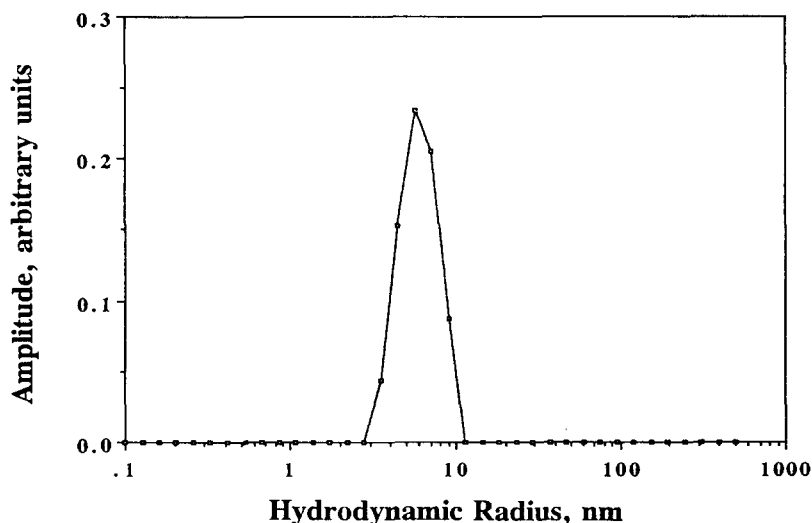


Fig. 3. CONTIN plot. Contributions to the total decay (amplitude in arbitrary units) are plotted as a function of the hydrodynamic radius  $R_h$  for  $5 \text{ mg ml}^{-1}$  solutions of S1 ( $37 \mu\text{M}$ ) at  $20^\circ\text{C}$  in  $10 \text{ mM KCl}$ ,  $10 \text{ mM Tris}$ ,  $2 \text{ mM MgCl}_2$  and  $0.25 \text{ mM EDTA}$  (pH 8). The scattering angle was  $90^\circ$ .

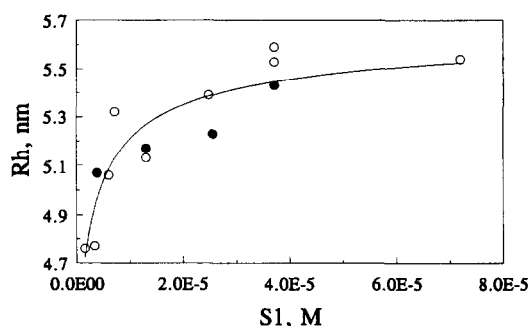


Fig. 4.  $R_h$  vs. [S1]. The values of  $R_h$ , averaged for all angles, are plotted against [S1] (open circles) and [S1·MgADP·P<sub>i</sub>] (filled circles). The full line is a fit to the combined data, assuming a monomer–dimer equilibrium.

$R_h$  increases with increasing [S1] (Fig. 4). The light scattering results are consistent with the steady state kinetic results, which were measured for the same four S1 preparations; both indicate that S1 aggregates. The data suggest that aggregation occurs independently of the presence of ATP. The increase in  $R_h$  with increasing [S1] was analyzed assuming that an S1 monomer–dimer equilibrium exists. The dissociation constant for the reaction was taken as  $K_D = [S1]^2/[S1_2]$ , and a quadratic equation was used to relate  $K_D$  to the fractions  $f_M$  and  $f_D$  of the total S1 concentrations [S1] and [S1<sub>2</sub>] respectively. The molecular weights of the S1 monomer and dimer were assumed to be proportional to the volumes  $V_M$  and  $V_D$  of the spherical hydrodynamic particles (i.e. to the cube of the observed hydrodynamic radii). The equation  $V_{OBS} = f_M \times V_M + f_D \times V_D$  (where  $V_{OBS}$  is the hydrodynamic volume calculated from the measured  $R_h$ ) was fitted to the data (Fig. 4) in order to obtain values for  $K_D$ ,  $V_M$  and  $V_D$ . For the best fit,  $K_D = 83 \mu\text{M}$  and  $V_D/V_M = 1.9$ . This analysis is a simplified version of the treatment used by Herbert and Carlson [27] to model the dimerization of myosin in high ionic strength solutions.

#### 4. Discussion

The kinetic data indicate that the apparent  $K_M$  for ATP and S1 increases with increasing [S1] (Fig. 1 and Fig. 2), which suggests that some type of S1–S1 interaction occurs at S1 concentrations as low as 5

$\mu\text{M}$ . The [S1] effect on  $K_M$  is small, but reproducible, and consistent with an earlier report of the  $K_M$  dependence on [S1] [28]. The analysis of the kinetic measurements made using enzyme concentrations at and above  $K_M$  is not straightforward [29]. Nonetheless, in the present case, it is not easy to propose reasonable explanations, other than changes in S1 aggregation, to explain the observed changes in the kinetic parameters occurring in response to increased [S1] (Fig. 1 and Fig. 2).

Polarized dynamic light scattering time correlation measurements provide a size-dependent physical parameter, the hydrodynamic radius  $R_h$ , which is sensitive to aggregation.  $R_h$  increases with [S1] (Fig. 4), indicating that S1 aggregates under these conditions and providing strong physical corroboration of the interpretation of the kinetic data. The CONTIN output of  $R_h$  lends itself to the use of the hydrodynamic volume to approximate the molecular weight of the scattering particles. The small size of S1 and its relatively globular shape justify using a simpler fitting procedure than that employed for the larger and more asymmetric myosin [27]. S1 aggregates larger than dimers were not considered because, for high [S1], the average  $R_h$  value appears (Fig. 4) to approach a constant magnitude (approximately 5.6 nm) close to  $2^{1/3}$  times the value observed for the lowest [S1] (approximately 4.7 nm). The ratio of the volumes of the equivalent hydrodynamic spheres of the presumed monomer and dimer, obtained from fitting the measured  $R_h$  vs. [S1] data, is  $V_D/V_M = 1.9$ , which justifies the assumption that aggregates larger than dimers can be ignored. The formation of dimers, rather than larger aggregates, suggests that the interactions between the S1 species may be specific. The best fit to the experimental increase in  $R_h$  with [S1] also provides an estimate of the dissociation constant,  $K_D = 83 \mu\text{M}$ . This result is consistent with a small amount of dimerization in the [S1] range for which  $K_M$  begins to increase (Fig. 1 and Fig. 2). The observed functional change in S1 as the concentration increases is consistent with the suggestion that dimerization is specific. Extrapolating the increase in the apparent  $K_M$  value observed in the low [S1] range to higher [S1]  $\approx K_D$  suggests that the apparent  $K_M$  could reach as high as 5  $\mu\text{M}$ .

Earlier reports of S1 dimerization from Morel and coworkers [18,19] are confirmed partially by the

light scattering and kinetic data presented here. Aggregates, which appear to be dimers, form as reported. On the other hand, the earlier reports indicated that nucleotide promoted dimerization and that the dimer enhanced MgATPase activity, neither of which was observed in the present study. Perhaps the differences are due to the S1 preparations. The earlier work was performed using S1 with only the essential light chain bound, and the present work was carried out using S1 with both essential and regulatory light chains present. Another potential explanation for the differences is the solution conditions. It should also be emphasized that, for different conditions from those used here, it is possible to prepare S1 which is free from detectable aggregates [30–32].

The kinetic data indicate that aggregated S1 does not have a different maximum activity, but has an increased apparent  $K_M$  for ATP (Fig. 1 and Fig. 2). The light scattering data show that ATP does not inhibit aggregation or dissociate the complex (Fig. 4). The increased apparent  $K_M$  for ATP, if it occurs in muscle, may be physiologically relevant. For example, if the two heads of myosin bind to one another during relaxation, they may have a reduced affinity for ATP. This may reduce ATP consumption under conditions of fatigue, for example. The change in  $K_M$  observed for isolated low [S1] in solution (Fig. 1) may appear to be too small to be relevant to muscle. However, the  $K_D$  value from the light scattering measurements suggests that the effect on  $K_M$  may be greater at higher [S1], and may be applicable to muscle.

### Acknowledgements

This work was supported by NIH grant AR42895 and NSF grant CHE 9520845.

### References

- [1] S.W. Provencher, *Comp. Phys. Comm.*, 27 (1982) 213–227.
- [2] S.W. Provencher, *Comp. Phys. Comm.*, 27 (1982) 229–242.
- [3] R. Cooke and K. Franks, *J. Mol. Biol.*, 120 (1978) 361–374.
- [4] Y.Y. Toyoshima, S.J. Kron, E.M. McNally, K.R. Niebling, C. Toyoshima and J.A. Spudich, *Nature*, 328 (1987) 536–539.
- [5] S. Lowey and K.M. Trybus, *Biophys. J.*, 68 (1995) 120S–127S.
- [6] R.W. Lymn and E.W. Taylor, *Biochemistry*, 10 (1971) 4617–4624.
- [7] D.D. Hackney, *Proc. Natl. Acad. Sci. USA*, 91 (1994) 6865–6869.
- [8] E. Berliner, E.C. Young, K. Anderson, H.K. Mahtani and J. Gelles, *Nature*, 373 (1995) 718–721.
- [9] S.P. Gilbert, M.R. Webb, M. Brune and K.A. Johnson, *Nature*, 373 (1995) 671–676.
- [10] T.Q.P. Uyeda, S.J. Kron and J.A. Spudich, *J. Mol. Biol.*, 214 (1990) 699–710.
- [11] C.R. Cremona, J.R. Sellers and K.C. Facemyer, *J. Biol. Chem.*, 270 (1995) 2171–2175.
- [12] M. Matsuura and M. Ikebe, *FEBS Lett.*, 363 (1995) 246–250.
- [13] H. Onishi and K. Fujiwara, *Biochemistry*, 29 (1990) 3013–3023.
- [14] H. Onishi, T. Maita, G. Matsuda and K. Fujiwara, *Biochemistry*, 28 (1989) 1905–1912.
- [15] K.K. Shukla, H.M. Levy, F. Ramirez and J.F. Marecek, *J. Biol. Chem.*, 263 (1988) 5049–5055.
- [16] H. Grussaute, F. Ollagnon and J.E. Morel, *Eur. J. Biochem.*, 228 (1995) 524–529.
- [17] R.J.C. Levine, R.W. Kensler, Z. Yang and H.L. Sweeney, *Biophys. J.*, 68 (1995) 224S.
- [18] J. Morel and M. Garrigos, *Biochemistry*, 21 (1982) 2679–2686.
- [19] N. Bachouchi, M. Garrigos and J.E. Morel, *J. Mol. Biol.*, 191 (1986) 247–254.
- [20] K.M. Nauss, S. Kitagawa and J. Gergely, *J. Biol. Chem.*, 244 (1969) 755–765.
- [21] S.S. Margossian and S. Lowey, *Methods Enzymol.*, 85 (1982) 55–71.
- [22] A.G. Weeds and R.S. Taylor, *Nature*, 257 (1975) 54–56.
- [23] K. Imamura, M. Tada and Y. Tonomura, *J. Biochem. (Tokyo)*, 59 (1966) 280–289.
- [24] M.A. Tracy and R. Pecora, *Macromolecules*, 25 (1992) 337–349.
- [25] S.S. Sorlie and R. Pecora, *Macromolecules*, 21 (1988) 1437–1449.
- [26] R. Pecora, *J. Phys. Chem.*, 48 (1968) 4126–4128.
- [27] T.J. Herbert and F.D. Carlson, *Biopolymers*, 10 (1971) 2231–2252.
- [28] D. Hackney and P.K. Clark, *J. Biol. Chem.*, 260 (1985) 5505–5510.
- [29] O.H. Strauss and A. Goldstein, *J. Gen. Physiol.*, 26 (1943) 559–585.
- [30] S. Highsmith and D. Eden, *Biochemistry*, 26 (1987) 2747–2750.
- [31] P.M. Curmi, D.B. Stone, D.K. Schneider, J.A. Spudich and R.A. Mendelson, *J. Mol. Biol.*, 203 (1988) 781–798.
- [32] K. Wakabayashi, M. Tokunaga, I. Kohno, Y. Sugimoto, T. Hamanaka, Y. Takezawa, T. Wakabayashi and Y. Amemiya, *Science*, 258 (1992) 443–447.